Is the In Vitro Ejection of Bacteriophage DNA Quasistatic? A Bulk to Single Virus Study

N. Chiaruttini,[†] M. de Frutos,[‡] E. Augarde,[†] P. Boulanger,[‡] L. Letellier,[‡] and V. Viasnoff[†*]
[†]Nanobiophysics Laboratory, Ecole Supérieure de Physique et de Chimie Industrielle, ParisTech, Centre National de la Recherche Scientifique, Paris, France; and [‡]Institut de Biochimie et Biophysique Moléculaire et Cellulaire, UMR 8619, Centre Nationale de la Recherche Scientifique, Université Paris Sud-11, Orsay, France

ABSTRACT Bacteriophage T5 DNA ejection is a complex process that occurs on several timescales in vitro. By using a combination of bulk and single phage measurements, we quantitatively study the three steps of the ejection—binding to the host receptor, channel-opening, and DNA release. Each step is separately addressed and its kinetics parameters evaluated. We reconstruct the bulk kinetics from the distribution of single phage events by following individual DNA molecules with unprecedented time resolution. We show that, at the single phage level, the ejection kinetics of the DNA happens by rapid transient bursts that are not correlated to any genome sequence defects. We speculate that these transient pauses are due to local phase transitions of the DNA inside the capsid. We predict that such pauses should be seen for other phages with similar DNA packing ratios.

INTRODUCTION

After more than two decades of scrutiny, the kinetic process for the internalization of the genome of a tailed bacteriophage into a host cell remains partially unexplained. It can be generically described by three stages. Bacteriophages first diffuse onto the host surface where they dock to a specific receptor (binding step). This docking triggers the opening of the capsid (channel opening step) and the transfer of the densely packed DNA from the capsid into the bacterium cytoplasm (DNA release step). The channel opening step involves conformational rearrangements of the protein complexes forming the tail tip, the tail tube, and the head-to-tail connector structure. Different physicochemical processes have been suggested to contribute to the driving force for the DNA transport. Among them: the active action of the viral/bacterial RNA polymerase (T7) (1) or the inner pressure exerted by the DNA highly compacted inside the capsid (2–4). In this study, we specifically focus on bacteriophage T5, a *Siphoviridae* phage infecting *Escherichia coli*. It differs from other members of this family such as λ and SPP1 by the large size of its dsDNA genome—121,750 bp (Genbank accession numbers: AY587007, AY692264, and AY543070T5) and of its icosahedral capsid, 90 nm in diameter. Pb5, the protein that binds to the outer membrane receptor protein FhuA (5,6), is located at the tip of the 170 nm long noncontractile tail.

The ability to trigger and follow in vitro the DNA ejection from some *Siphoviridae* phages (λ, T5, SPP1) allowed the study of the different stages of this process by bulk measurements and single phage assays. The dependence of the bulk ejection kinetics was determined in vitro as a function of receptor concentration (5), temperature (7–9), salt (10), and medium osmotic pressure (2,11–13). Much attention has been devoted to quantitatively measure the ejection process and model it (14–20), considering the inner capsid pressure as the major driving force for ejection. Observations of DNA release at the single phage level revealed that the process is fast (~60 kbp/s) (21) and salt-dependent (17). The release occurs continuously for phage λ (17) and by discrete bursts for phage T5 (21). For phage λ, the release speed of single DNA molecules does not vary monotonically with the inner capsid fraction of genome as expected from the inner pressure calculation at equilibrium. Instead, a nonmonotonic friction coefficient, varying over two orders of magnitude as a function of DNA ejected length, was postulated to describe the DNA ejection process (17).

In this article, we provide the first study to our knowledge that quantitatively addresses the phage ejection process over all involved timescales by reconstructing the bulk behavior of a phage assembly from single phage assays. We quantitatively determine the kinetics of each of the three DNA ejection steps. We report that T5 DNA is indeed ejected by short-lived bursts that do not correlate with single strand interruptions in the genome as previously postulated (9,21). Based on our results and recent cryo-EM microscopy studies (22), we propose that the DNA ejection process in vitro is nonquasistatic and that the driving force of the ejection is largely reduced from its equilibrium value by the existence of local phase transitions of the inner capsid DNA during the ejection. We eventually show that these transient pauses in the ejection process are not readily related to the unique in vivo two-step transport process of T5 (23–25). During the first step transfer (FST), the first 8% of the genome are internalized in the bacterial host. Then a pause of a few minutes occurs during which viral proteins are produced, allowing inactivation/modification of host functions and completion of DNA transfer (second step transfer,

Submitted January 27, 2010, and accepted for publication April 12, 2010.

*Correspondence: virgile.viasnoff@espci.fr

Editor: Catherine A. Royer.

0006-3495/10/07/0447/9 $2.00

doi: 10.1016/j.bpj.2010.04.048

SST) (26). In vitro, locations of the pauses are not unique and their lifetimes are much shorter.

MATERIALS AND METHODS

T5 strains

T5st(0), a heat stable deletion mutant (114 kbp, Genbank Acc AY692264) containing four single-strand interruptions in its genome, was compared to the nickless mutant T5amHA911 (121 kbp) (27). Both phages were produced on the host strain *E. coli* F and purified on Cesium Chloride gradients (28). They were stored in phage buffer (100 mM NaCl, 1 mM $MgSO_4$, 1 mM $CaCl_2$, and 10 mM Tris-HCl, pH 7.6). The final titers were 1.10^{13}/mL and 2.10^{12}/mL for T5st(0) and T5amHA911, respectively. The absence of nicks in the T5amHA911 DNA was checked by pulse-field gel electrophoresis (see Fig. S1 in the Supporting Material).

FhuA

The gene encoding the outer membrane protein FhuA was overexpressed in *E. coli* HO830 transformed with plasmid pHX405 and the protein was purified by using the protocol previously described (5). FhuA was stored at a concentration of 50 μM in 20 mM Tris-HCl buffer pH 7.8, containing 250 mM NaCl, and 1% Octyl-β-D-glucopyranoside (OG).

Fluorometry bulk assays

Bulk fluorescence measurements of DNA ejection were performed with a Fluoromax-4 spectrofluorimeter (HORIBA Jobin Yvon, Edison, NJ) in a 1 × 0.4 cm quartz cuvette at 37°C or 24°C. The excitation and emission wavelengths were set at 498 and 520 nm, respectively, and slits were 2 nm for excitation and emission. SYBR Green I (10,000× in dimethyl sulfoxide; Invitrogen, Carlsbad, CA) was used as the groove-binding DNA dye. It was diluted 4000-fold in 150 μL of phage buffer supplemented with 0.03% lauryldimethylamine *n*-oxide (LDAO), a detergent that maintains FhuA in a soluble condition. We checked that the use of OG instead of LDAO leads to the same results. We also checked that the concentration of dye did not limit the measurement of the ejection kinetics. A quantity of 1.5 μL of phage T5 at a concentration of 10^{11}/mL was added to a final concentration of 10^9/mL. The resulting fluorescence was set as the background. After 5 min, 8 μL of FhuA was added and stirred to trigger the ejection. To reduce light exposure, acquisition points were taken every 10 s (exposure time: 0.5 s). All experiments were performed under these conditions unless otherwise noted.

Light-scattering bulk assays

Light-scattering experiments were carried out on a homemade setup as previously described (9). We used a He-Ne laser (632.8 nm) and a thermostated cell placed at the center of a goniometer. Samples (300 μL) were prepared by dilution of phage particles and receptors in phage buffer supplemented with 0.03% LDAO. OG could not be used because it forms micelles that contribute to the scattered signal. The final concentrations in the assays were 10^{10}/mL for T5st(0) and 130 nM for FhuA. DNA ejection triggered by the addition of FhuA defined the time origin. Scattering intensity was recorded at an angle equal to 90° from the incident laser beam and the temperature was fixed at 37°C.

Single virus studies

Single virus assays were performed on an inverted microscope (Axioplan; Carl Zeiss, Jena, Germany), with a 40× water objective (NA 1.2). The fluorescence illumination source was a 120-W UVICO 2000 lamp (Rapp Opto-Electronic, Hamburg, Germany). The images were acquired by an iXon EMCCD camera (Andor Technology, Belfast, Northern Ireland). The temperature was fixed at 24°C (±0.2°C).

Phages at a concentration of 10^{11}/mL were incubated with FhuA (5 μM) for 5 min at 4°C in phage buffer supplemented with 1% OG. Under these conditions, phages bind to their receptor but do not eject their DNA (5,28). This suspension was diluted 1000-fold before it was introduced into the chilled flow chamber (uncoated μ-slide VI; Ibidi, Eching, Germany). Thirty seconds were necessary to obtain a suitable density of phages adsorbed on the surface. The channel was subsequently flushed with phage buffer supplemented with a 1000-fold dilution of SYBR Green I and with 1% OG. As a result, both unattached phage particles and FhuA molecules were removed. An oxygen scavenging system containing Glucose Oxydase (cat. No. G2133; Sigma, St. Louis, MO) at 3 mg/mL, Catalase (cat. No. C100; Sigma) at 1.5 mg/mL, Glucose (20%), and Dithiothreitol (cat. No. 43815; Sigma) at 150 mM was also diluted 10 times in the previous buffer to prevent photodamage. The temperature was then raised to 24°C to initiate DNA ejection. At this point, we used different protocols for the long-time population study and for the high-speed DNA release study.

For long-time single virus population study, we briefly adjusted the focus under continuous illumination at the beginning of the experiment, while the rest of the kinetics was followed for 1 h with only 20 snapshots of 0.1 s exposure time. The illumination was synchronized with the image acquisition to prevent photodamage. The illumination power was set as low as possible, provided that individual DNA spots remained clearly visible. Note that in this configuration, the concentration of Tris-HCl in the phage buffer was 100 mM rather than 10 mM, to prevent the buffer acidification due to the oxygen scavenging system. The release of individual DNA molecules was visualized by the appearance of distinguishable individual fluorescent spots.

For high-speed movies of DNA release, illumination was continuous and set at full intensity. The camera was operated in a 2 × 2 pixels binned mode, thus reaching a 62-fps acquisition rate. A flow of phage buffer containing OG was applied at a rate of 300 μL/min, corresponding to a shear rate of 53 s^{-1}, to keep the stretched ejected DNA molecules in focus. We analyzed the movies by measuring the integrated fluorescence intensity for each released DNA molecule using a home-developed ImageJ macro (Image J; National Institutes of Health, Bethesda, MD). To enhance the signal/noise ratio, the integration area was optimized to the apparent size of the DNA molecule. We also subtracted the background signal, as measured from an area near the processed DNA. The ejection velocities were accurately computed by filtering the data with the nonlinear filtering skim described in Haran (29). The derivative of the fluorescence intensity increase was calculated over eight points (130 ms).

RESULTS

As a start, we coarse-modeled the full ejection kinetics by a series of three successive steps:

$$\varphi + \underbrace{FhuA \xrightarrow{k_b} \varphi}_{\text{Phage binding}}\ \underbrace{FhuA \xrightarrow{k_{op}} \varphi}_{\text{Channel opening}}\ \underbrace{FhuA^* \xrightarrow{k_{re}} \varphi FhuA_e}_{\text{DNA release}} + DNA.$$

The first step corresponds to the binding of the phage φ to its receptor FhuA with a typical rate k_b. This binding triggers conformational changes in the phage tail that are transmitted to the head-to-tail connector, allowing its opening. This channel opening step is characterized by a rate of activation k_{op}. At this stage the phage-FhuA complex (φFhuA*) is ready for DNA release. During the third step, the DNA is released into the external medium leaving the capsid $\varphi FhuA_e$ empty. We first oversimplify the release process and reduce

its kinetics to a typical rate k_{re}. Bulk measurements and single virus assays were used to measure the kinetic rates of each step.

First, we measure the binding rate of FhuA to the bacteriophage by monitoring the dependence of the kinetics on the receptor concentration. Then, we show that in the regime of high receptor concentration, the bulk kinetics probes only the channel opening step. By using single virus assays, we eventually report that the DNA release proceeds by rapid stochastic bursts of partial ejection.

Determination of the binding kinetic constant of phage T5 to FhuA

The overall ejection process can be followed by measuring the bulk fluorescence increase of the groove binding dye SYBR Green I which stains, selectively, the ejected fraction of DNA. Indeed, control experiments (Fig. 1) show that the dye hardly stains or permeates the capsid in the absence of FhuA. Furthermore, the DNA staining outside the capsid was checked to be instantaneous and constant during the course of an experiment. We first measured the binding rate of phage T5 to FhuA by monitoring the dependence of the kinetics on the receptor concentration. Bacteriophage T5st(0) was added at a concentration of 10^9 particles/mL (~1 pM) whereas the concentration of receptor [FhuA] was varied from 300 pM to 80 nM leading to a receptor/phage ratio higher than 300 for all experiments. As both FhuA and the dye are in large excess, their concentrations remain constant during the course of an experiment. The kinetics of the binding step is thus expected to be of the first order with a binding rate $k_1 = k_b[\text{FhuA}]$ that depends linearly on [FhuA]. (This assumes that FhuA molecules in solution are all functional and monomeric. Our measurements hence provide a lower bound for the value of k_b.) On the other hand, the channel opening and DNA release steps are independent of [FhuA]. For the sake of simplicity, we reduced all kinetic events that do not depend on FhuA concentration to a single kinetic event with a rate k_{out}. The ejection process is thus simplified to the following model:

$$\varphi + FhuA \xrightarrow{k_b} \varphi FhuA \xrightarrow{k_{out}} \varphi FhuA_e + DNA.$$

The resulting analytical expression for the time dependence of ejected DNA in the solution is a sum of a concave exponential rise due to the faster rate and a convex exponential increase due to the slower rate. It reads as

$$DNA(t,[FhuA]) = 1 - \frac{1}{1 - r[FhuA]} \times \left(e^{-k_b[FhuA]t} - r[FhuA]e^{-k_{out}t}\right) \text{ with } r = \frac{k_b}{k_{out}}. \quad (1)$$

Equation 1 can thus be used to fit the fluorescence increase at various FhuA concentrations. Fig. 1 shows the global DNA ejection kinetics for five FhuA concentrations probed by bulk fluorescence measurements. All curves are normalized to the fluorescence intensity at saturation. For k_b [FhuA] >> k_{out}, i.e., for large concentrations of FhuA (10 nM, 80 nM), the kinetics of the ejection saturates and becomes FhuA-independent. In this limit, the apparent rate of the ejection (defined as the inverse of the time needed to eject half of the final amount of DNA) is k_{out}. Conversely, for low receptor concentrations (but still at large receptor to phage ratio), the apparent rate is significantly slower and depends on [FhuA]. In this regime, the total ejection is dominated by the binding to FhuA and not by the channel opening or the DNA release step. A global fit of the ejection kinetics for this set of five concentrations with Eq. 1 leads to the following values of the kinetic constants: $k_b = 3.10^6\ \text{M}^{-1}\ \text{s}^{-1}$ and $k_{out} = 4.5\ 10^{-3}\ \text{s}^{-1}$ at 37°C. The high value of k_b, in line with typical rates of fast protein-protein interactions (30), is consistent with previous results showing that the T5 tail protein pb5 binds with high affinity to FhuA in vitro (31). The proposed model oversimplifies the ejection kinetics and works best in the limit where the binding step is rate-limiting as exemplified by the better quality of the fit for low FhuA concentrations (Fig. 1). However, models that are more complex do not significantly affect the determination of k_b (data not shown). Note that, in the rest of the article, the

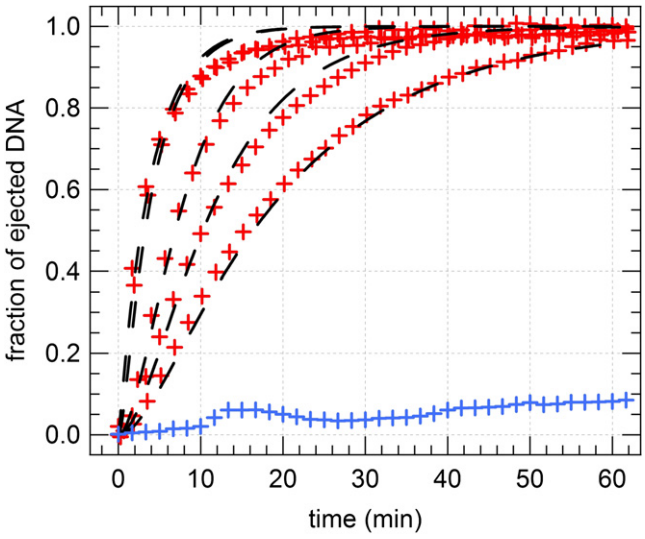

FIGURE 1 Time-dependence of the ejected fraction of T5st(0) DNA, measured by bulk fluorometry at 37°C with SYBR Green I at various FhuA concentrations. At $t = 0$, the ejection is triggered by the addition of FhuA to the solution, except for the blue curve where no FhuA is added (negative control). The fraction of DNA is equal to the ratio of the fluorescence increase to the final fluorescence intensity once the background is subtracted. Five different FhuA concentrations are represented: 0.3 nM, 0.6 nM, 1 nM, 10 nM, and 80 nM (*red symbols* from *bottom* to *top*). At low receptor concentrations, the kinetics is dominated by the binding step, whereas at high receptor concentration, the kinetics saturates to a limit curve. Note that the kinetics for [FhuA] = 10 nM and [FhuA] = 80 nM can hardly be distinguished, despite an eightfold increase in receptor concentration. (*Black dashed curves*) Global fits of the data to the theoretical expression in Eq. 1. We find a binding kinetic constant $k_b = 3.10^6\ \text{M}^{-1}\ \text{s}^{-1}$.

ejection kinetics will always be studied in the limit of high [FhuA], thus eliminating the binding step from the kinetic measurements. In the next section, we further refine our model and we show that a single rate k_{out} is not enough to describe the kinetics in the high [FhuA] regime.

Kinetics of the channel opening step: bulk and single virus analysis

In a previous work (9), the kinetics of T5st(0) DNA ejection was monitored by the decay of the light scattered at a fixed angle by the encapsidated DNA. Fluorometry and light scattering are complementary assays as the fluorescence measures the amount of DNA expelled from the phages whereas light scattering is sensitive to the amount of DNA remaining in the capsids. Additional to this, light scattering measurements are independent of any added external dye.

Fig. 2 represents the kinetics of ejection measured with both methods at 37°C and in the limit of high FhuA concentration. As already reported (9), both methods show a double timescale behavior. A convex double-exponential fit of the data in this regime (not to be confounded with the two exponentials defined in Eq. 1) gives the following values of the two characteristic times: $\tau_{fast} = 120$ s, $\tau_{slow} = 540$ s for fluorometry; $\tau_{fast} = 120$ s, $\tau_{slow} = 780$ s for light scattering. The overall agreement for both methods is good despite a small discrepancy in the longest characteristic time τ_{slow}. Note also that both the nicked T5st(0) and nickless T5amHA911 strains display the same global ejection kinetics.

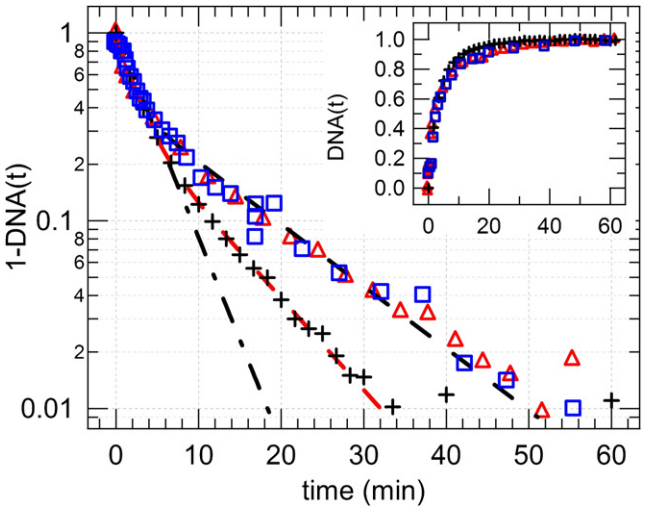

FIGURE 2 Bulk T5st(0) DNA ejection kinetics in the high [FhuA] limit. (*Inset*) Comparison between ejection kinetics measured by fluorometry (+) or light scattering (□) methods at 37°C. The light-scattering kinetics of the nickless strain amHA911 is also shown (△). The ejection is triggered by addition of a saturating concentration of FhuA. All curves are normalized. (*Main graph*) Linear-log representation of the same data set. The first minutes of the kinetics are well fitted by a simple exponential (*slashed dotted line*). Double-exponential fits are necessary to fit the entire kinetic process measured by fluorometry and by light scattering (*red dashed* and *black dashed lines*, respectively).

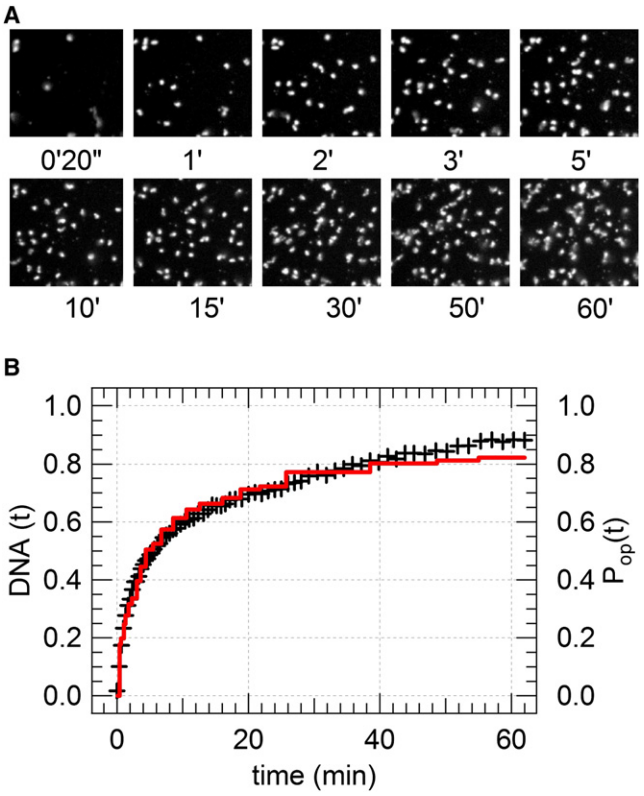

FIGURE 3 Comparison between bulk ejection kinetics DNA(t) (+), and the probability of ejection determined by single virus experiments (*line*) at 24°C, $P_{op}(t)$. (*A*) Single virus assay: snapshots of a typical field of view showing DNA ejection from single viruses. The appearance of each spot corresponds to a single DNA release event. (*B*) The ejection kinetics measured by fluorometry in the limit of high FhuA concentration (+) overlays the time dependence of the DNA ejection probability measured at the single phage level (*line*).

To investigate the contribution of the channel opening step and DNA release step to the observed bulk kinetics, we performed single virus fluorescence assays. The kinetics of DNA ejection of individual virus particles adsorbed on a hydrophobic surface in a flow chamber was recorded (Fig. 3 *A*) and the bulk behavior was deduced from the statistical distribution of single ejection events (Fig. 3 *B*). SYBR Green I was used to stain the ejected DNA in conjunction with an oxygen-scavenging system that reduces photodamage. T5 particles were incubated for 5 min with their receptors at 4°C. This low temperature incubation allows the phage to bind to FhuA, but inhibits all subsequent ejection steps for ~30 min (9). The phages were then adsorbed for 30 s on the chilled chamber surface that was subsequently flushed to get rid of unadsorbed phages and unbound receptor proteins. The ejection process of adsorbed phages was triggered by a temperature jump to 24°C. Fluorescent spots of DNA appeared over time on the microscope field of view, each spot corresponding to a single ejected DNA molecule (Fig. 3 *A*). These DNA spots were never observed with the phage alone (data not shown). As detailed in the next

section, the recording of the fluorescence increase of each individual spots showed that the full genome length was ejected within a few seconds. However, there was an average lag time of several minutes between the temperature jump and the initiation of DNA release. The DNA release step is thus more than one-order-of-magnitude faster than the channel opening step. This observation is consistent with previous results obtained with phage λ (17).

The probability of DNA ejection of a phage, $P_{op}(t)$, was measured as a function of the time t elapsed since the temperature jump and was compared to the ensemble kinetics determined by fluorometry. To do this, we counted the number of ejection events in a 200 μm $\times$ 200 μm field of view as a function of t. Time-lapse experiments were performed over a period of 1 h. Snapshots of 0.1 s exposure time were taken at increasing time intervals as shown on Fig. 3 *A*. The time dependence of the probability of ejection $P_{op}(t)$ could be measured although the DNA release step appeared instantaneous at this frame rate. Fig. 3 *B* shows that $P_{op}(t)$ overlays with the normalized bulk fluorescent measurement of the whole ejection process at high concentration of receptors. This result implies that the kinetics measured by bulk assays cannot account for the DNA release but reflects only the dynamics of the conformational changes during the channel opening step. This result will be further commented upon in the Discussion.

Fast DNA release kinetics with short lived pauses

We further focused on the fast kinetics step of DNA release that occurs once the channel is open. We recorded the fluorescence signal of the DNA released by single bacteriophages as a function of time. We used a mild flow (shear rate 53 s^{-1}) to slightly stretch the DNA exiting from the capsid and to keep it in focus. We monitored the integrated intensity along the DNA length as a function of time at a frame rate of 62 images/s. In contrast with previous work (17), we did not measure the linear length of the DNA stretched in the flow but we estimated the arc length of the DNA by measuring the total fluorescence intensity of the mildly stretched molecule. The validity of this approach was confirmed by using test DNA molecules (see Fig. S3). For bacteriophage T5st(0), we found that the DNA length released when the total fluorescence intensity reached its steady value was equal to the DNA contour length (39 μm) once the various elongation factors (staining and flow stretch) were taken into account (see Supporting Material). Measuring the fluorescence intensity has an improved resolution over direct length measurements, allowing a precision of 2 kb pairs at a video rate of 62 frames/s (Fig. 4 *A*). Fig. 4 *B* shows four characteristic traces of the ejected length $l(t)$ for phage T5st(0) and T5amHA911 as a function of time. Both phages showed similar ejection patterns with short pauses of a few seconds. The dependence of the speed $V_{\text{eject}}(l)$ with the amount of ejected T5st(0) DNA was then extracted.

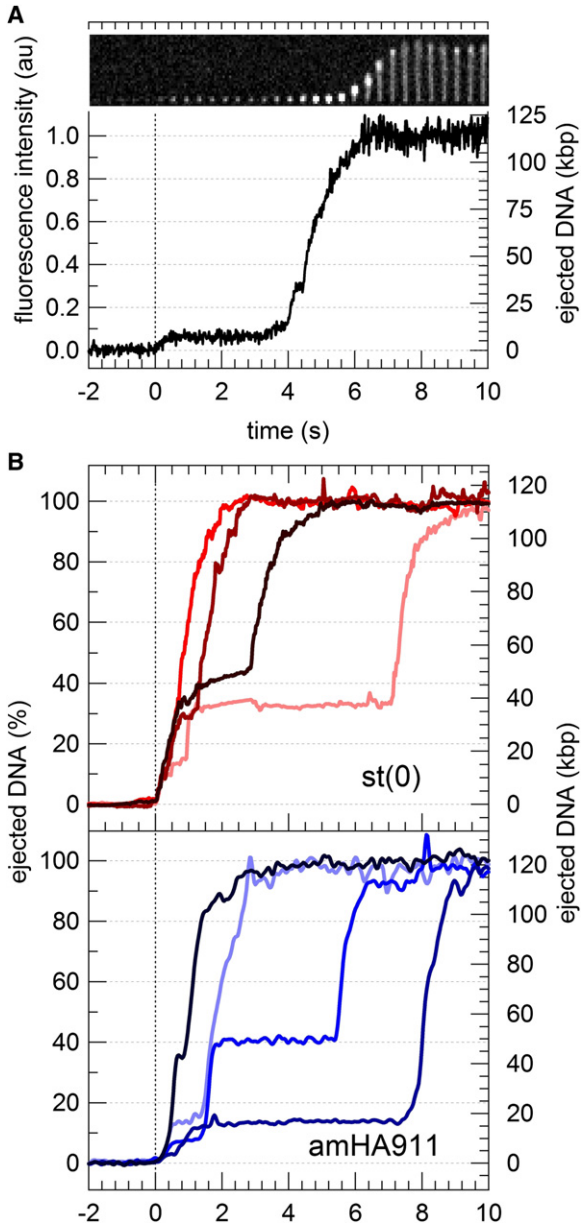

FIGURE 4 Fast DNA release kinetics of single T5st(0) phages. (*A*) Time series of a single phage releasing its DNA. At $t = 0$, the DNA channel opens and the release begins. Only 1 in every 24 images of the 62-fps movie is shown for clarity. The length of the ejected DNA (*line*) is computed through the normalized total fluorescence intensity of the phage elongated in the mild buffer flow. Note that the fluorescence increase is not synchronized to the DNA extension in the flow. (*B*) Four typical traces of DNA release displaying slow partial ejections and pauses for T5st(0). Same curves for T5amHA911.

A typical example is given in Fig. 5 *A*. The average (62 traces) release time for the full 114-kbp genome was 8 s with a distribution ranging from 3 to 20 s. The mean velocity of 14 kbp/s corresponds to a release rate two-orders-of-magnitude higher than the channel opening rate. Reducing the DNA release step to a single constant rate $k_{re} = 1/8$ s is enough to justify why the bulk measurements probe

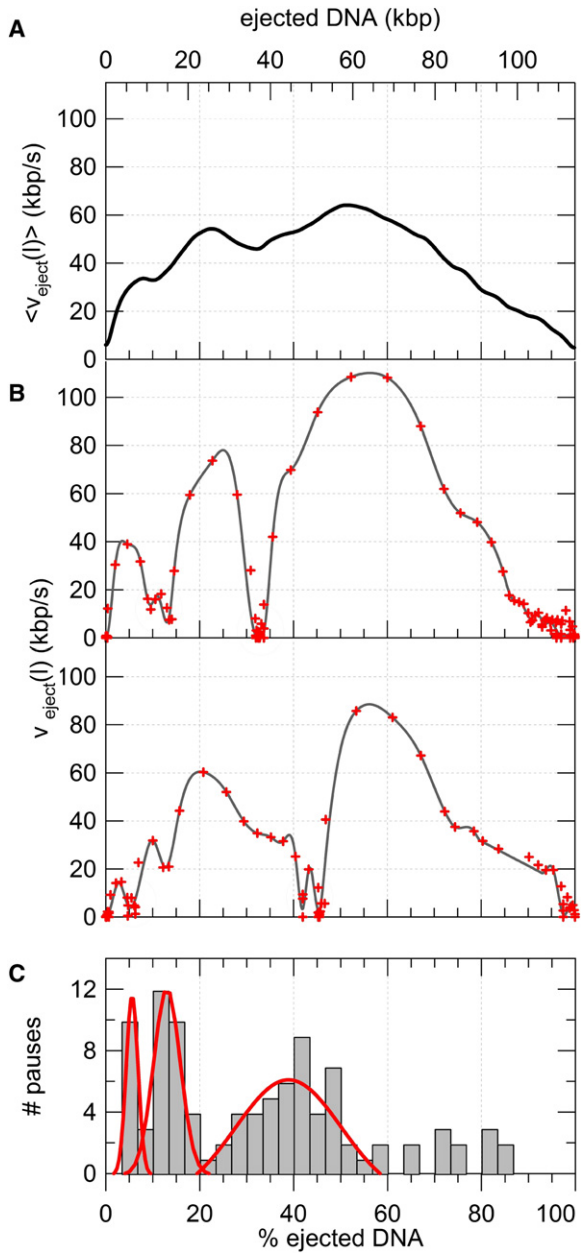

FIGURE 5 (*A*) Event-averaged DNA release velocity as a function of ejected DNA length. Note the nonmonotonic behavior of the velocity. (*B*) Two individual velocity traces calculated from a single phage ejection. Note the appearance of regions with zero velocity corresponding to pauses. (*C*) Histogram of the pauses location along the genome. We determine one peaked region at 6% ± 1%, and two broader regions at 12% ± 4% and 40% ± 12%.

only the channel opening process. However, it does not accurately describe the DNA release process. First, the ejection velocity $\langle V_{\text{eject}}(l)\rangle$ averaged over all events does not vary linearly or even monotonically with the length l of ejected DNA. This result is shown on Fig. 5 *A* and corroborates what was observed for λ phages (17): $\langle V_{\text{eject}}(l)\rangle$ increases until approximately half of the genome is ejected and then decays to zero until the release is completed. Second, this population trend is modulated at the level of single virus ejection by the presence of stochastic bursts of partial ejection followed by transient pauses for ~90% of the phages (Fig. 5 *B*). The maximum ejection speed during a burst ranges between 60 and 120 kbp/s and the pauses occur at rather defined lengths of the ejected genome. This is shown on Fig. 5 *C* where the histogram of the pause locations displays the three most preferred lengths: 6% ± 1%, 12% ± 4%, 40% ± 12%. This steplike ejection contrasts with the reported continuous ejection of phage λ. The origin of these pauses will be further commented upon in the Discussion.

DISCUSSION

Our results provide a comprehensive picture of the in vitro ejection process of bacteriophage T5 DNA from ensemble studies to single phage assay. We first characterized each of the three steps of DNA ejection (receptor binding, channel opening, and DNA release) by their typical rate k_b, k_{op}, and k_{re}, respectively. Using a combination of bulk and single virus measurements we could address each step separately and quantitatively estimate the values of $k_b = 3.10^6\ \text{M}^{-1}\ \text{s}^{-1}$ (37°C), $k_{op} = 4.5\ 10^{-3}\ \text{s}^{-1}$ (37°C) or $1.6\ 10^{-3}$ (24°C), and $k_{re} = 1.25\ 10^{-1}\ \text{s}^{-1}$ (24°C). However, our study revealed that 1), the channel opening step is characterized not by one, but by at least two, timescales; and 2), the release of DNA occurs by a series of bursts of partial ejection with an unexpected dependence of the ejection speed with the fraction of ejected genome. In this section, we discuss the origin of these two observations. A comparison with previous publications reporting pauses in T5 ejections can be found in the Supporting Material.

The three steps of the ejection process must occur sequentially. As a result, the overall kinetics is dominated by the slowest process. The binding rate depends on [FhuA]. At low FhuA concentrations, the binding events can be made rate-limiting. The bulk kinetics then probes mostly the kinetics of FhuA binding to the phages. Conversely, at high receptor concentration, the binding rate can be very fast compared to the two other processes. Moreover, our single molecule studies also show that the channel opening step is much slower than the complete DNA release process ($k_{op} << k_{re}$). It results that, in the limit of high [FhuA], the overall kinetics probed by bulk measurements is dominated by the channel opening step as demonstrated by the overlay of this kinetics with the channel opening probability measured at the single phage level. This conclusion falls along the lines of results reported for λ and SPP1 (8,17).

Another piece of evidence that leads to the same conclusion is the following. The bulk ejection kinetics was probed by fluorescence measurements under appropriate conditions where the fluorescence increase is directly proportional to the total amount of ejected basepairs. On the other hand, when measured by light scattering, the signal is sensitive to the DNA inside the capsid and varies with the square of the total

mass of the phage (including DNA) (8). The good agreement between the normalized signals obtained by both techniques indicates that the DNA is either fully in or fully out of the capsid on the timescales probed by bulk measurements. This agreement also shows that the dye does not influence the ejection process and that the previous studies using light scattering actually probed the channel opening step and not the bursts of partial ejections during the DNA release, as had been postulated (9). Then how can the complex kinetics of the channel opening step be explained? The existence of two rearrangement timescales τ_{fast} and τ_{slow} (Fig. 2) suggests two main parallel pathways for this opening. Each pathway corresponds to a succession of events triggered by the binding to the receptor that may include transmission of an opening signal to the head-to-tail connector, connector opening, rearrangements, and release of specific tail proteins (8,32,33). Any of these structural events can be limiting for the opening. According to this interpretation, the probability for each pathway is given by the weight of each exponential term in the fit. By using the fluorometry data, we found that the pathways corresponding to τ_{fast} and τ_{slow} contribute to 60% ± 3% and 40% ± 3% of the ejections, respectively. However, our results do not determine whether these pathways are due to an alternative series of intermediate states within each phage or originate from variability within the phage population (34).

Another point we want to address is the intermittent behavior of the DNA release. The DNA release step can be described at three levels of increasing precision. The first level consists of the assumption of a single ejection rate $k_{re} = 1.25\ 10^{-1}\ s^{-1}$. As for phage λ, we found that this rate is large compared to the other rates involved in the total ejection process. Because the DNA release occurs basepair-after-basepair at a finite speed, the description of the process as a single kinetic step is not accurate.

We can further refine our model based on a more mechanistic description. As the Reynolds number of the ejection is low ($Re \sim 10^{-10}$), the viscous drag force $\eta \cdot v_{eject}$ should instantaneously equilibrate the ejection driving force F_{drive}. This driving force is expected to decrease monotonically with the amount of encapsidated DNA. Indeed, at equilibrium the ejection driving force should be equal to the restoring force acting against the DNA encapsidation for a given value of packaged DNA. This force was measured for ϕ29, T4, and λ (4,35,36). It monotonically increases with the amount of encapsidated DNA. The main contribution to this restoring force is thought to originate from the interstrand electrostatic repulsion brought in close proximity by the capsid confinement (18,20,37,38). Assuming a constant viscous drag, the velocity is thus expected to decrease continuously with the amount of ejected DNA. This is not the case for our observations. Indeed, the ensemble-averaged ejection velocity is small when the ejection starts and gradually increases up to 60–120 kbp/s at ~50% of the ejected genome as also observed for phage λ (typically 60 kbp/s) (17). The velocity eventually decays to zero as the ejection proceeds. Grayson et al. (17) explained this behavior by introducing a friction coefficient that depends on the ejected length. The interstrand friction inside the capsid is assumed to depend on the degree of compaction of the DNA inside the capsid.

In addition, a recent cryo-EM study (22) suggested that the DNA inside the T5 capsid is not organized as a inverse spool as supposed by Grayson et al. (17) but as nanodomains of hexagonal DNA crystals with a three-dimensional lattice of topological defects. As the capsid empties, the packaged DNA always occupies the full inner volume but undergoes a series of phase transitions of local ordering until it reaches an isotropic distribution when ~60% of the genome is released. In the case of the packaging process, the speed is slow enough (10–100 bp/s) for us to expect that the resisting force equals the quasistatic value F_{eq} calculated as the gradient of the equilibrium packing free energy with respect to the packaged DNA length. On the contrary, the ejection process is three orders of magnitude faster (10^5, 10^4 bp/s). One can conjecture that collective relaxation processes of the nanodomains are slower than the ejection process. In that case, the local pinning of the DNA configuration states can lower the force driving the ejection below its quasistatic value F_{eq}. Although, from a phenomenological point of view, this effect may be described as a force-dependent friction, we believe that the nonmonotonic behavior of the speed originates, at least partly, from the out-of-equilibrium value of the driving force.

Our interpretation is further supported by the presence of pauses during the ejection observed for 90% of the phage population under our experimental conditions. In a previous work, Mangenot et al. (21) already reported the existence of pauses during the ejection of phage T5 DNA using a similar single phage technique and putatively attributed them to the presence of single strand interruptions on the genome. We have revisited these observations/interpretations based first on the availability of the nickless amber mutant T5amHA911 and second on the improved detection and analysis scheme which gives both better localization of the pauses and the time dependence of each single ejection event. T5amHA911 and T5st(0) displayed similar bulk kinetics of DNA ejection and similar pauses in the individual DNA ejections. This is indeed expected from our conclusion that the bulk kinetics reflects only the channel opening step and indicates that the presence of the nicks is not critical to trigger pauses. In conclusion, there should be no relation between the genomic position of the nicks and the localization of the ejection pauses. As a possible explanation, we hypothesize that delays in local phase transition and topological defect pinning at large packing ratios are responsible not only for the slow-down of the ejection process but also for the existence of pauses in a stick-slip manner. Some simulations (19,39) nonetheless report that at moderate packing ratios, the steric hindrances due to topological knots do not result in the arrest of the ejection.

The analysis of the time course of each individual ejection process indicated that although the pauses occur with a random probability, they are mainly localized in three regions of the genome: 6% ± 1%; 12% ± 4%; and 40% ± 12%. Note that we measure an increasing spread of the pausing regions with their increasing position on the genome. The pause at ~6% is defined within the precision of our detection. The large spread of the other pauses further demonstrates that the stalling, at least for the pauses in the second and third region, originates neither from a genetically encoded defect nor from a specific sequence effect. In addition, the multimodal distribution of pause location mainly located within the first 50% of the genome rules out the possibility of a random gating of the ejection complex channel. We thus speculate that the origin of the pauses lies in the local structure of the DNA spooling that can be reinforced by DNA/capsid interactions and/or specific local organization. This point is further supported by the following observation. According to Leforestier et al. (12), the DNA in the capsid adopts a loose isotropic conformation once ~65% of the genome is ejected. In parallel, we hardly see any pauses above 60% and the average speed decays almost linearly with the ejected length above this limit. In the loose isotropic configuration, the driving force should be closer to its equilibrium value. If these transient stops are due to local rearrangements within the phage head, we expect other phage strains with a similar packing density to also display transient ejection stops when observed with the same accuracy.

Finally, we point out that the presence of these pauses during an in vitro ejection should not be readily related to the existence of the two-step ejection in vivo. Indeed the pauses observed between the ejection of the FST and SST DNA were measured in bulk and last ~5–10 min (24,40). We never observed any so-long-lived pause in vitro. On the contrary, the steps that we observe in the in vitro ejection are too short-lived to be observed by bulk in vivo measurements. Hence, the relevance of the observed pauses and their relationship with the FST and SST steps observed in vivo is still an open question.

SUPPORTING MATERIAL

Three figures are available at http://www.biophysj.org/biophysj/supplemental/S0006-3495(10)00546-1.

We thank Eric Raspaud for his technical support and his participation in preliminary light-scattering data acquisition, and R. Phillips for fruitful discussions. The T5amHa911 mutant was kindly provided by I. Molineux.

Funding was provided by the ANR program No. ANR-06-PCVI-0002, the Centre National de la Recherche Scientifique program ''Prise de Risque'', and the Centre de Compétence NanoSciences Ile de France. N.C. acknowledges financial support from the French Ministry of Research.

REFERENCES

1. Molineux, I. J. 2001. No syringes please, ejection of phage T7 DNA from the virion is enzyme driven. *Mol. Microbiol.* 40:1–8.
2. Evilevitch, A., L. Lavelle, …, W. M. Gelbart. 2003. Osmotic pressure inhibition of DNA ejection from phage. *Proc. Natl. Acad. Sci. USA.* 100:9292–9295.
3. Riemer, S. C., and V. A. Bloomfield. 1978. Packaging of DNA in bacteriophage heads: some considerations on energetics. *Biopolymers.* 17:785–794.
4. Smith, D. E., S. J. Tans, …, C. Bustamante. 2001. The bacteriophage straight φ29 portal motor can package DNA against a large internal force. *Nature.* 413:748–752.
5. Boulanger, P., M. le Maire, …, L. Letellier. 1996. Purification and structural and functional characterization of FhuA, a transporter of the *Escherichia coli* outer membrane. *Biochemistry.* 35:14216–14224.
6. Mondigler, M., R. T. Vögele, and K. J. Heller. 1995. Overproduced and purified receptor binding protein pb5 of bacteriophage T5 binds to the T5 receptor protein FhuA. *FEMS Microbiol. Lett.* 130:293–300.
7. Löf, D., K. Schillén, …, A. Evilevitch. 2007. Forces controlling the rate of DNA ejection from phage λ. *J. Mol. Biol.* 368:55–65.
8. Raspaud, E., T. Forth, …, M. de Frutos. 2007. A kinetic analysis of DNA ejection from tailed phages revealing the prerequisite activation energy. *Biophys. J.* 93:3999–4005.
9. de Frutos, M., L. Letellier, and E. Raspaud. 2005. DNA ejection from bacteriophage T5: analysis of the kinetics and energetics. *Biophys. J.* 88:1364–1370.
10. Evilevitch, A., L. T. Fang, …, C. M. Knobler. 2008. Effects of salt concentrations and bending energy on the extent of ejection of phage genomes. *Biophys. J.* 94:1110–1120.
11. Castelnovo, M., and A. Evilevitch. 2007. DNA ejection from bacteriophage: towards a general behavior for osmotic-suppression experiments. *Eur Phys J E Soft Matter.* 24:9–18.
12. Leforestier, A., S. Brasilès, …, F. Livolant. 2008. Bacteriophage T5 DNA ejection under pressure. *J. Mol. Biol.* 384:730–739.
13. São-José, C., M. de Frutos, …, P. Tavares. 2007. Pressure built by DNA packing inside virions: enough to drive DNA ejection in vitro, largely insufficient for delivery into the bacterial cytoplasm. *J. Mol. Biol.* 374:346–355.
14. Ali, I., D. Marenduzzo, and J. M. Yeomans. 2008. Ejection dynamics of polymeric chains from viral capsids: effect of solvent quality. *Biophys. J.* 94:4159–4164.
15. Arsuaga, J., and Y. Diao. 2008. DNA knotting in spooling like conformations in bacteriophages. *Comput. Math. Meth. Med.* 9:303–316.
16. Evilevitch, A., M. Castelnovo, …, W. M. Gelbart. 2004. Measuring the force ejecting DNA from phage. *J. Phys. Chem. B.* 108:6838–6843.
17. Grayson, P., L. Han, …, R. Phillips. 2007. Real-time observations of single bacteriophage-λ DNA ejections in vitro. *Proc. Natl. Acad. Sci. USA.* 104:14652–14657.
18. Inamdar, M. M., W. M. Gelbart, and R. Phillips. 2006. Dynamics of DNA ejection from bacteriophage. *Biophys. J.* 91:411–420.
19. Matthews, R., A. A. Louis, and J. M. Yeomans. 2009. Knot-controlled ejection of a polymer from a virus capsid. *Phys. Rev. Lett.* 102: 088101–088104.
20. Purohit, P. K., M. M. Inamdar, …, R. Phillips. 2005. Forces during bacteriophage DNA packaging and ejection. *Biophys. J.* 88:851–866.
21. Mangenot, S., M. Hochrein, …, L. Letellier. 2005. Real-time imaging of DNA ejection from single phage particles. *Curr. Biol.* 15:430–435.
22. Leforestier, A., and F. Livolant. 2010. The bacteriophage genome undergoes a succession of intracapsid phase transitions upon DNA ejection. *J. Mol. Biol.* 396:384–395.
23. Lanni, Y. T. 1960. Invasion by bacteriophage T5. II. Dissociation of calcium-independent and calcium-dependent processes. *Virology.* 10:514–529.
24. Lanni, Y. T. 1968. First-step-transfer deoxyribonucleic acid of bacteriophage T5. *Bacteriol. Rev.* 32:227–242.
25. Lanni, Y. T., D. J. McCorquodale, and C. M. Wilson. 1964. Molecular aspects of DNA transfer from phage T5 to host cells. 2. Origin of first-step-transfer DNA fragments. *J. Mol. Biol.* 10:19–27.

26. McCorquodale, J. D., and H. R. Warner. 1988. Bacteriophage T5 and related phages. *In* The Viruses. R. Calendar, editor. Plenum Press, New York.

27. Rogers, S. G., E. A. Godwin, …, M. Rhoades. 1979. Interruption-deficient mutants of bacteriophage T5. I. Isolation and general properties. *J. Virol.* 29:716–725.

28. Boulanger, P. 2009. Purification of bacteriophages and SDS-PAGE analysis of phage structural proteins from ghost particles. *Methods Mol. Biol.* 502:227–238.

29. Haran, G. 2004. Noise reduction in single-molecule fluorescence trajectories of folding proteins. *Chem. Phys.* 307:137–145.

30. Northrup, S. H., and H. P. Erickson. 1992. Kinetics of protein-protein association explained by Brownian dynamics computer simulation. *Proc. Natl. Acad. Sci. USA.* 89:3338–3342.

31. Plançon, L., C. Janmot, …, P. Boulanger. 2002. Characterization of a high-affinity complex between the bacterial outer membrane protein FhuA and the phage T5 protein pb5. *J. Mol. Biol.* 318:557–569.

32. Boulanger, P., P. Jacquot, …, L. Letellier. 2008. Phage T5 straight tail fiber is a multifunctional protein acting as a tape measure and carrying fusogenic and muralytic activities. *J. Biol. Chem.* 283:13556–13564.

33. Plisson, C., H. E. White, …, E. V. Orlova. 2007. Structure of bacteriophage SPP1 tail reveals trigger for DNA ejection. *EMBO J.* 26: 3720–3728.

34. Hulen, C., B. Labedan, and J. Legault-Demare. 1980. Evidence for heterogeneity in populations of T5 bacteriophage. II. Some particles are unable to inject their second-step-transfer DNA. *J. Virol.* 36: 633–638.

35. Fuller, D. N., D. M. Raymer, …, D. E. Smith. 2007. Measurements of single DNA molecule packaging dynamics in bacteriophage λ reveal high forces, high motor processivity, and capsid transformations. *J. Mol. Biol.* 373:1113–1122.

36. Fuller, D. N., D. M. Raymer, …, D. E. Smith. 2007. Single phage T4 DNA packaging motors exhibit large force generation, high velocity, and dynamic variability. *Proc. Natl. Acad. Sci. USA.* 104:16868–16873.

37. Fuller, D. N., J. P. Rickgauer, …, D. E. Smith. 2007. Ionic effects on viral DNA packaging and portal motor function in bacteriophage ϕ29. *Proc. Natl. Acad. Sci. USA.* 104:11245–11250.

38. de Frutos, M., S. Brasiles, …, E. Raspaud. 2005. Effect of spermine and DNase on DNA release from bacteriophage T5. *Eur Phys J E Soft Matter.* 17:429–434.

39. Marenduzzo, D., E. Orlandini, …, C. Micheletti. 2009. DNA-DNA interactions in bacteriophage capsids are responsible for the observed DNA knotting. *Proc. Natl. Acad. Sci. USA.* 106:22269–22274.

40. Bonhivers, M., and L. Letellier. 1995. Calcium controls phage T5 infection at the level of the *Escherichia coli* cytoplasmic membrane. *FEBS Lett.* 374:169–173.